

Drift Velocity and Anisotropy of Hot Electrons in *n* Germanium

H. G. REIK AND H. RISKEN
Philips Research Laboratories, Aachen, Germany

(Received January 22, 1962)

The drift velocity and the angle between the direction of the drift velocity and the electric field are calculated as a function of the electric field strength, the crystal orientation, and the lattice temperature. The fit between experimental and theoretical results is nearly quantitative. By the process of fitting, the optical deformation potential constant D_0 and the intervalley rate constant w_2 are determined. The values $D_0 = 0.5 \times 10^9$ eV/cm and $1.66 \times 10^{10} \text{ sec}^{-1} \leq w_2 \leq 10^{11} \text{ sec}^{-1}$ are consistent with the results of independent experiments.

I. INTRODUCTION

THE electric conduction in *n*-type germanium at high electric fields shows quite distinct deviations from the low-field Ohmic behavior. The tensor of differential mobility becomes nondiagonal and field dependent. The diagonal elements decrease with increasing electric-field strength. Under the same conditions, the ratios of nondiagonal to diagonal elements tend, roughly speaking, to field-independent finite values. In accordance with this, the following facts have been found experimentally: (1) With increasing field, the drift velocity approaches a field-independent saturation value.^{1,2} (2) The absolute value of the drift velocity and the way in which it is approached, depend distinctly on the crystal orientation.³ (3) In general, the electric field strength and the drift velocity are not parallel (Sasaki effect). The angle ψ between these vectors depends on the crystal orientation and is zero in the simplest crystallographic directions only.⁴⁻⁶

A theory of these hot electron effects requires that the structure of the conduction band of germanium be known, at least for those parts of the Brillouin zone which are accessible to electrons for the experimental conditions under study. Furthermore, for the same conditions, the distribution of the electrons must be given.

In this paper, we replace the required knowledge of the band structure by the assumption that even under hot electron conditions only the $\langle 111 \rangle$ valleys of germanium are populated. Furthermore we assume that the effective masses are constants for the average energies of the electrons under consideration. For this special model of the band structure, the distribution of hot electrons can be obtained by solution of the Boltzmann equation as shown previously.⁷ In this paper, this distribution function will be used for the calculation of the drift velocity and the anisotropy of

hot electrons. It will be shown that a nearly quantitative fit between the theoretical formulas for the many-valley model of the band structure and the experimental results for *n*-Ge is possible. Moreover, the values of the optical deformation potential constant D_0 and the intervalley rate constant w_2 determined by the process of fitting, are consistent with the results of other independent experiments. The possibility of a consistent fit seems to indicate that the assumptions and approximations, inherent in this and the previous paper, are not unreasonable.

The procedure for obtaining these results is as follows: In Sec. II a convenient form of the general expression for the drift velocity is given and the previous results for the electron distribution are summarized. In Sec. III the drift velocity and anisotropy are calculated for a special electron distribution, which leads to simple results. In Secs. IV and V, the general case is treated. An explanation of the field dependence of the Sasaki effect is given and the comparison between theory and experiment is carried out. Section VI finally deals with the influence of approximations on the interpretation of the experimental results in the framework of the many-valley model and with the question of the reliability of the whole theory.

II. EXPRESSIONS FOR THE DRIFT VELOCITY AND THE DISTRIBUTION FUNCTION OF HOT ELECTRONS

The average drift velocity \mathbf{v}_d of an electron distribution in a many-valley semiconductor is by definition given by

$$\mathbf{v}_d = \frac{\sum_j \int \mathbf{v}^{(j)} f^{(j)}(\Delta \mathbf{k}^{(j)}) d^3 \Delta \mathbf{k}^{(j)}}{\sum_l \int f^{(l)}(\Delta \mathbf{k}^{(l)}) d^3 \Delta \mathbf{k}^{(l)}}, \quad (1)$$

where the sums extend over all valleys. Here $\Delta \mathbf{k}^{(j)}$ is the wave vector of an electron, reckoned from the energy minimum of the valley j , $f^{(j)}(\Delta \mathbf{k}^{(j)})$ is the distribution function, and $\mathbf{v}^{(j)}$ denotes the group velocity.

We shall now write Eq. (1) in a form in which immediate use can be made of the distribution functions derived previously.⁷ For this reason, we transform the

¹ E. J. Ryder and W. Shockley, Phys. Rev. **81**, 139 (1951).

² E. J. Ryder, Phys. Rev. **90**, 766 (1953).

³ M. I. Nathan, Bull. Am. Phys. Soc. **5**, 194 (1960).

⁴ W. Sasaki and M. Shibuya, J. Phys. Soc. Japan **11**, 1202 (1956).

⁵ W. Sasaki, M. Shibuya, and K. Mizuguchi, J. Phys. Soc. Japan, **13**, 456 (1958).

⁶ W. Sasaki, M. Shibuya, K. Mizuguchi and G. M. Hatoyama, J. Phys. Chem. Solids **8**, 250 (1959).

⁷ H. G. Reik and H. Risken, Phys. Rev. **124**, 777 (1961).

surfaces of constant energies to spheres in each particular valley by means of the transformation of Herring and Vogt⁸ by which effective wave vectors $\Delta\mathbf{k}^{*(i)}$ are introduced instead of $\Delta\mathbf{k}^{(i)}$, and effective fields $\mathbf{F}^{*(i)}$ instead of \mathbf{F} . The effective vectors are defined by

$$\Delta\mathbf{k}^{*(i)} = [\tilde{\alpha}^{(i)}]^\frac{1}{2} \Delta\mathbf{k}^{(i)}, \quad (2)$$

$$\mathbf{F}^{*(i)} = [\tilde{\alpha}^{(i)}]^\frac{1}{2} \mathbf{F}, \quad (3)$$

and $\tilde{\alpha}$ is the tensor of the reciprocal effective mass times the free electron mass. In the new variables the distribution function can be written in the form⁷

$$f^{(i)}(\Delta\mathbf{k}^{*(i)}) = \sum_l f_l^{(i)}(\epsilon) P_l(\cos\vartheta),$$

where ϑ is the angle between the effective field and the effective wave vector, and ϵ is the energy of the electrons. Consequently, the following expression for the drift velocity is obtained instead of (1):

$$\mathbf{v}_d = \frac{1}{3} \left(\frac{2}{m_0} \right)^\frac{1}{2} \frac{\sum_j \int_0^\infty \epsilon f_1^{(j)}(\epsilon) d\epsilon [\tilde{\alpha}^{(j)}]^\frac{1}{2} \mathbf{F}_0^{*(j)}}{\sum_l \int_0^\infty \epsilon^\frac{1}{2} f_0^{(l)}(\epsilon) d\epsilon}. \quad (4)$$

Here m_0 is the free electron mass, and $\mathbf{F}_0^{*(i)}$ is the unit vector in the direction of the effective field. In this relation, our previous results for $f_0^{(i)}(\epsilon)$ and $f_1^{(i)}(\epsilon)$ can be immediately used. On the one hand, this is done by means of the equation^{9,10}

$$f_1^{(i)}(\epsilon) = E_{\langle\tau\rangle}^{*(i)} (df_0^{(i)}/d\epsilon), \quad (5)$$

where $E_{\langle\tau\rangle}^{*(i)}$ is the energy fed to an electron by the electric field during the relaxation time $\langle\tau\rangle$ for momentum scattering. The energy $E_{\langle\tau\rangle}^{*(i)}$ depends on the value of the effective field in the valley under consideration on account of the relations

$$E_{\langle\tau\rangle}^{*j} = E_{\langle\tau\rangle} F^{*(j)}/F, \quad (6)$$

where

$$E_{\langle\tau\rangle} = eF\langle\tau\rangle(2\epsilon/m_0)^\frac{1}{2}, \quad (7)$$

and

$$\langle\tau\rangle = \frac{\rho \hbar^4 c_l^2}{\sqrt{2} 2^4 \pi^3 m_l m_t^\frac{1}{2} \Xi_1^2 k T_{\text{eff}} \epsilon^\frac{1}{2}}. \quad (8)$$

Here m_l and m_t are the longitudinal and the transverse masses, ρ is the density, c_l is the longitudinal velocity of sound, and Ξ_1 is the acoustical deformation potential constant for momentum scattering. Expression (8) is formally identical with the expression for the acoustical relaxation time for momentum scattering [Eq. 10(a) of reference 7], apart from the fact that in (8) the

temperature T is replaced by the effective temperature

$$T_{\text{eff}} = T$$

$$+ \frac{D_0^2 \hbar c_l^2}{\Xi_1^2 2 k \omega_0} \left[(2n_q + 1) + (N - 1) \frac{D_i^2 \omega_0}{D_0^2 \omega_i} (2n_i + 1) \right]. \quad (9)$$

Here N is the number of valleys in the band under study; n_q and n_i are the number of optical and intervalley phonons; ω_0 and ω_i are their frequencies; and D_0 and D_i are the deformation potential constants for interactions of the electrons with them. The replacement of T by T_{eff} in Eq. (8) is due to the fact that for hot electrons with average energies larger than $\hbar\omega_0$ and $\hbar\omega_i$ the emissive interactions of electrons with these high-energy phonon fully contribute to the momentum relaxation.

As $\langle\tau\rangle$ varies as $\epsilon^{-\frac{1}{2}}$, $E_{\langle\tau\rangle}$ is independent of the energy. Consequently, insertion of (5) and (6) into (4) leads to the final expression for the drift velocity:

$$\mathbf{v}_d = -\frac{1}{3} \left(\frac{2}{m_0} \right)^\frac{1}{2} E_{\langle\tau\rangle} \frac{\sum_j \int_0^\infty f_0^{(j)}(\epsilon) d\epsilon \tilde{\alpha}^{(j)} \mathbf{F}_0}{\sum_l \int_0^\infty \epsilon^\frac{1}{2} f_0^{(l)}(\epsilon) d\epsilon}, \quad (10a)$$

or

$$\mathbf{v}_d = -\frac{1}{3} \left(\frac{2}{m_0} \right)^\frac{1}{2} E_{\langle\tau\rangle} \sum_j \left\{ \frac{n_j \int_0^\infty f_0^{(j)}(\epsilon) d\epsilon}{n \int_0^\infty \epsilon^\frac{1}{2} f_0^{(i)}(\epsilon) d\epsilon} \tilde{\alpha}^{(j)} \mathbf{F}_0 \right\}. \quad (10b)$$

where

$$\frac{n_j}{n} = \frac{\int_0^\infty \epsilon^\frac{1}{2} f_0^{(j)}(\epsilon) d\epsilon}{\sum_l \int_0^\infty \epsilon^\frac{1}{2} f_0^{(l)}(\epsilon) d\epsilon}, \quad (11)$$

in which now only integrals over $f_0^{(i)}(\epsilon)$ are contained.

For these functions, results have been obtained in three cases: (1) The energy loss of the electrons is almost entirely due to optical intravalley scattering; intervalley scattering is completely absent. (2) Intervalley scattering is strong enough to establish a steady-state distribution of the electrons in the different valleys, although the electron transfer still does not affect the energy balance. (3) The transfer of electrons between different valleys caused by intervalley scattering has an influence on the energy balance comparable to the influence of the interactions of electrons with optical phonons.

In cases 1 and 2, a Maxwellian distribution

$$f_0^{(j)}(\epsilon) = C_j \exp(-\beta_j \epsilon), \quad (12)$$

with $\beta_j = 1/kT_e^{*(j)}$ given by

$$\beta_j = [E_{\tau_0}^{*(j)} E_{\langle\tau\rangle}^{*(j)} / \hbar\omega_0 + \hbar\omega_0(n_q + \frac{1}{2})]^{-1}, \quad (13)$$

is found as a solution of the Boltzmann equation.

⁸ C. Herring and E. Vogt, Phys. Rev. **101**, 944 (1956).

⁹ E. M. Conwell, Phys. Rev. **123**, 454 (1961).

¹⁰ Compare Eq. (15) of reference 7.

Here $E_{\tau_0}^{*(i)}$ is the energy gain during the optical time of energy relaxation,

$$\tau_0 = \frac{\rho \hbar^3 \omega_0}{3\sqrt{2} 2^2 \pi^2 m_i m_l^{\frac{1}{2}} D_0^2 \epsilon^{\frac{1}{2}}}. \quad (14)$$

Cases 1 and 2 are therefore only to be distinguished by the different dependence of C_j on the electron temperature. In case 1, all the valleys have the same population and consequently $C_j \propto \beta_j^{\frac{1}{2}}$ on account of the normalization condition. In case 2, however, a finite repopulation

$$\frac{n_j}{n} = \frac{\beta_j^{\frac{1}{2}} [1 - \hbar \omega_i \beta_j / 2(2n_i + 1)]^{-1}}{\sum_l \beta_l^{\frac{1}{2}} [1 - \hbar \omega_i \beta_l / 2(2n_i + 1)]^{-1}}, \quad (15)$$

$$C_j \propto \beta_j^2 [1 - \hbar \omega_i \beta_j / 2(2n_i + 1)]^{-1}, \quad (16)$$

is set up. In case 3, finally, the transfer of electrons also does affect the form of the energy distribution of the electrons $f_0^{(i)}(\epsilon)$, which is no longer Maxwellian but is found to be

$$f_0^{(i)}(\epsilon) = \left\{ K_j - \bar{\gamma} \beta_j C \left[(N-1) \beta_j \epsilon + \sum_{l \neq j} \left(\frac{\beta_l}{\beta_j - \beta_l} - \int_0^\epsilon \frac{\exp[(\beta_j - \beta_l) \xi] - 1}{\xi} d\xi \right) \right] \right\} \times \exp(-\beta_j \epsilon) + \bar{\gamma} \beta_j C \sum_{l \neq j} \frac{\beta_l}{\beta_j - \beta_l} \exp(-\beta_l \epsilon), \quad (17)$$

where

$$\bar{\gamma} = D_i^2 (2n_i + 1) / D_0^2 \hbar \omega_i, \quad (18)$$

$$K_j = C \{ \beta_j^2 [1 - \beta_j \hbar \omega_i / 2(2n_i + 1)]^{-1} - 2\bar{\gamma} \beta_j^2 \sum_l [1/\beta_l - 1/\beta_j] - \bar{\gamma} \beta_j \sum_l \ln(\beta_j/\beta_l) \}. \quad (19)$$

The transport properties of hot electrons with these different types of electron distributions will now be studied.

III. TRANSPORT PROPERTIES OF HOT ELECTRONS IN A SIMPLE CASE

In this section the properties of hot electrons whose energy distribution is a Maxwellian one will be treated for the range of high-electric fields, where $\beta_j = 1/kT_e^{*(i)}$ is approximately given by

$$\beta_j = \hbar \omega_0 / E_{\tau_0}^{*(i)} E_{(\tau)}^{*(i)}, \quad (20)$$

which means that the second term in Eq. (13) has been neglected. The dependence of the electron temperature on the electric field strength and the field direction is especially simple in this case. Making use of (6) and (7) and of (8), (9), and (14), β_j can be written as a

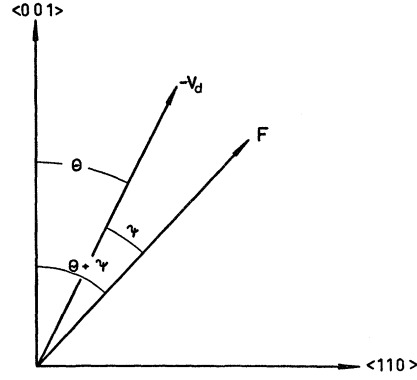


FIG. 1. Definition of the angles in the Sasaki plane.

product of two factors,

$$\beta_j = \frac{\hbar \omega_0}{E_{\tau_0} E_{(\tau)}} \times \frac{F^2}{[F^{*(i)}]^2} = \frac{96[m_0^2 \Xi_1 D_0]^2 k T_{\text{eff}}}{[e F \rho c \hbar^3]^2 (\det \tilde{\alpha})^2} \times \frac{F^2}{[F^{*(i)}]^2}. \quad (21)$$

The first of these factors is the same for all valleys and depends only on the electric field and the lattice temperature. On account of (3), the second factor,

$$[F/F^{*(i)}]^2 = 1/(\mathbf{F}_0 \tilde{\alpha}^{(i)} \mathbf{F}_0), \quad (22)$$

describes the influence of the field direction on the electron temperature in the particular valley under study. This factor is in general different for different valleys.

If repopulation is taken into account in a way consistent with the approximation (20), the distribution of the electrons over the different valleys is given by

$$n_j/n = \beta_j^{\frac{1}{2}} / \sum_l \beta_l^{\frac{1}{2}}, \quad (23)$$

which is identical with the well-known Knudsen distribution in very dilute gases. On account of (21) and (22), the distribution of the electrons depends only on the field direction:

$$n_j/n = (\mathbf{F}_0 \tilde{\alpha}^{(i)} \mathbf{F}_0)^{-\frac{1}{2}} / \sum_l (\mathbf{F}_0 \tilde{\alpha}^{(l)} \mathbf{F}_0)^{-\frac{1}{2}}. \quad (24)$$

For field directions confined to the $\langle 110 \rangle$ plane (see Fig. 1), the repopulation (24) as a function of the field direction is plotted in Fig. 2.

Insertion of (12), (21), and (22) into (10b) leads to the following expression for the drift velocity¹¹:

$$\mathbf{v}_d = -\frac{2}{3} \left(\frac{2\hbar \omega_0 \langle \tau \rangle}{\pi m_i \tau_0} \right)^{\frac{1}{2}} \mathbf{S} = -\frac{D_0}{\Xi_1 \pi^{\frac{1}{2}} (3m_i k T_{\text{eff}})^{\frac{1}{2}}} \mathbf{S}, \quad (25)$$

¹¹ H. G. Reik, H. Risken, and G. Finger, Phys. Rev. Letters **5**, 423 (1960).

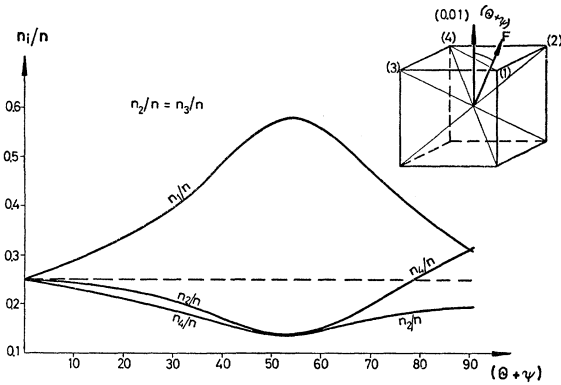


FIG. 2. Population ratios n_i/n vs field direction $\Theta + \psi$ according to (24).

where the direction-dependent part \mathbf{S} is given by

$$\mathbf{S} = \left(\frac{m_t}{m_0} \right)^{\frac{1}{2}} \sum_j \left\{ \frac{n_j}{n} \frac{\tilde{\alpha}^{(j)} \mathbf{F}_0}{(\mathbf{F}_0 \tilde{\alpha}^{(j)} \mathbf{F}_0)^{\frac{1}{2}}} \right\}. \quad (26)$$

While the vector \mathbf{S} is independent of the absolute value of the electric field strength as well as of the lattice temperature, the drift velocity decreases with increasing lattice temperature. The explanation of the saturation of the drift velocity as due to the energy loss of the electrons by interactions with the optical phonons was put forward by Shockley.^{12,13} Since then, the question of the relative contribution of the different scattering mechanisms to the losses under a variety of conditions has been studied extensively.¹⁴⁻²¹

The properties of the relation (26) are plotted in Figs. 3-5, where full curves refer to the Knudsen distribution, (23) and (24), broken curves to no repopulation, $n_j/n = \frac{1}{3}$. In Fig. 3 the dependence of the absolute value of \mathbf{S} (and therefore of the absolute value of \mathbf{v}_d) on the field direction, the so-called longi-

¹² W. Shockley, Bell System Tech. J. **30**, 990 (1951).

¹³ Shockley calculated the drift velocity under the assumption of infinitely strong interactions between electrons and optical phonons for a monoenergetic electron distribution and a needle distribution in k space. In both of these cases he found $v_d \approx (\hbar\omega_0/m^*)^{\frac{1}{2}}$. A Shockley type of formula,

$$\mathbf{v}_d = -2 \left(\frac{2}{3\pi} \right)^{\frac{1}{2}} \left(\frac{\hbar\omega_0}{m_t} \right)^{\frac{1}{2}} \frac{1}{(2n_q + 1)^{\frac{1}{2}}} \mathbf{S},$$

is also obtained from (25) and (9) for $D_0/\mathcal{E}_1 \rightarrow \infty$. This does not mean infinitely strong optical interaction, for β_j is now given by

$$\beta_j = 3 \frac{\hbar}{\omega_0} \left[\frac{4\pi^2 D_0^2}{\rho \hbar^3 e F} \right]^2 \frac{m_0^3}{\det \tilde{\alpha}} \frac{m_0}{\mathbf{F}_0 \tilde{\alpha}^{(j)} \mathbf{F}_0} (2n_q + 1),$$

and for the applicability of the theory $\beta_j < 1/\hbar\omega_0$ is required.

¹⁴ J. Yamashita and M. Watanabe, Progr. Theoret. Phys. (Kyoto) **12**, 443 (1954).

¹⁵ B. V. Paranjape, Proc. Phys. Soc. (London) **B70**, 628 (1957).

¹⁶ E. M. Conwell, J. Phys. Chem. Solids **8**, 234 (1959).

¹⁷ E. M. Conwell, Bull. Am. Phys. Soc. **5**, 61 (1960).

¹⁸ E. M. Conwell and A. L. Brown, Phys. Chem. Solids **15**, 208 (1960).

¹⁹ K. H. Seeger, Z. Physik **156**, 582 (1959).

²⁰ A. F. Gibson, J. W. Granville, and E. G. S. Paige, J. Phys. Chem. Solids **19**, 198 (1961).

²¹ M. A. C. S. Brown, J. Phys. Chem. Solids **19**, 218 (1961).

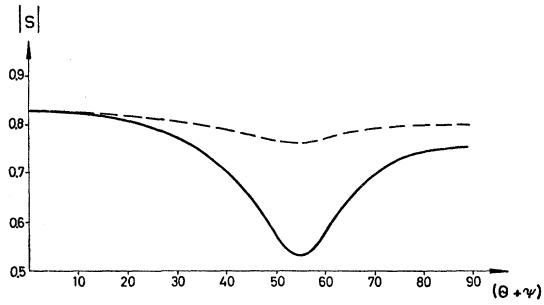


FIG. 3. Variation of the absolute magnitude of the drift velocity with the field direction $\Theta + \psi$ (longitudinal anisotropy) according to Eqs. (25) and (26).

tudinal anisotropy is given. In Figs. 4 and 5 the angle ψ between the direction of the drift velocity and the electric field, the so-called transverse anisotropy, is plotted against field direction and sample orientation, respectively.

The results of our theory for the simple case under study, with repopulation taken into account, agree quite remarkably with most of the experimental results. An indirect confirmation of Eqs. (23) and (24) is due to Paige.²² In his work, an analysis of Koenig's experimental results on the anisotropy of hot electrons,²³ based on Stratton's transport theory²⁴ (in which also a Maxwellian energy distribution for each valley is used), was given. For $F = 1000$ v/cm, Paige's analysis, as far as the repopulation is concerned is summarized in Table I and compared to the results of Eq. (24). (See also Fig. 2).

A number of direct confirmations exist for Eq. (26) with repopulation taken into account. According to Fig. 2 the ratio of the drift velocities in the $\langle 001 \rangle$

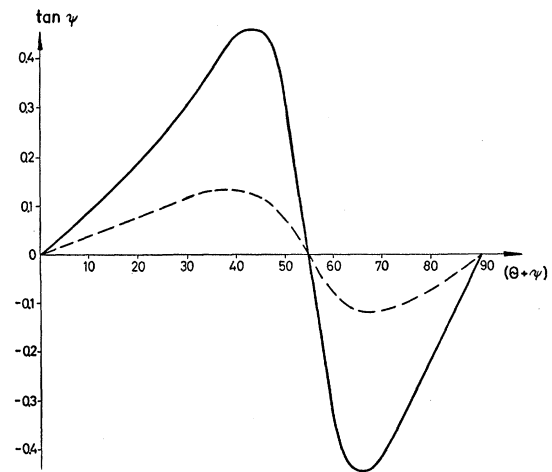


FIG. 4. Anisotropy angle ψ vs field direction $\Theta + \psi$ according to (26).

²² E. G. S. Paige, Proc. Phys. Soc. (London) **B75**, 174 (1960).

²³ S. H. Koenig, Proc. Phys. Soc. (London) **B73**, 959 (1960).

²⁴ R. Stratton, Proc. Roy. Soc. (London) **A242**, 355 (1957).

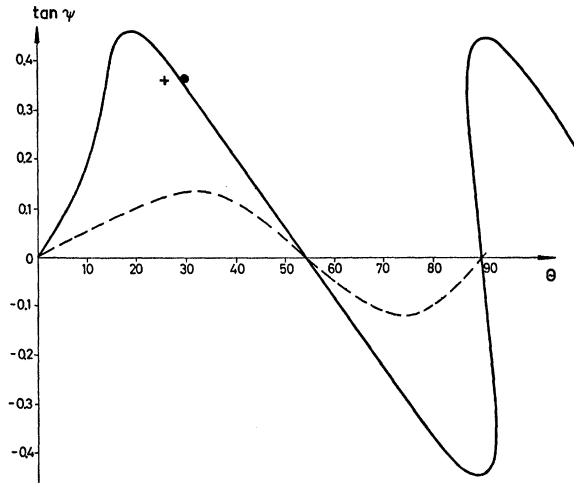


FIG. 5. Anisotropy angle ψ vs sample orientation Θ . ●—measurement of Koenig *et al.*,²⁶ $F=4000$ v/cm; $T=80^\circ\text{K}$; +—measurement of Schmidt-Tiedemann²⁶; $F=3500$ v/cm; $T=78^\circ\text{K}$.

and $\langle 111 \rangle$ directions $v_{d\langle 001 \rangle}/v_{d\langle 111 \rangle}=1.58$, whereas for $F=1000$ v/cm, $T=78^\circ\text{K}$, $v_{d\langle 001 \rangle}/v_{d\langle 111 \rangle}=1.60$ was found by Nathan.³ Experimental results on the anisotropy angle ψ , obtained by Koenig, Nathan, Paul, and Smith²⁵ and by Schmidt-Tiedemann²⁶ are given in Fig. 5. The results of these authors are close to the theoretical curve. Finally, Eq. (25) gives the correct temperature dependence of the saturation drift velocity in contradistinction to Shockley's results.^{12,13}

The optical deformation potential constant can therefore be evaluated from measurements of the saturation drift velocity using (25). For the evaluation a value $|S|=0.80$ and $\Xi_1=11$ ev (calculated with $\Xi_u=17$ ev, $\Xi_d=-5.8$ ev has been used. The result is shown in Table II. (Koenig's values of v_d are calculated from measurements of the saturation current density.)

The values of D_0 are consistent with the analysis of mobility data by Brooks.²⁷ They are of the same order of magnitude as a value given by Meyer,^{28,29} $D_0=1.15 \times 10^9$ ev/cm, which was extracted from experi-

TABLE I. Repopulation of hot electrons according to Paige^a and to Eq. (24).

Experimental conditions and results (Koenig ^b)			
$\Theta=26^\circ$, $T=78^\circ\text{K}$, $F=1000$ v/cm, $\psi=11^\circ$, $\Theta+\psi=37^\circ$			
Analysis	n_1/n	$n_2/n=n_3/n$	n_4/n
Paige ^a	0.46	0.18	0.18
Eq. (24)	0.46	0.19	0.16

^a E. G. S. Paige, Proc. Phys. Soc. (London) **75**, 174 (1960).

^b H. Koenig, Proc. Phys. Soc. (London) **73**, 959 (1959).

²⁵ S. H. Koenig, M. I. Nathan, W. Paul, and A. C. Smith, Phys. Rev. **118**, 1217 (1960).

²⁶ K. J. Schmidt-Tiedemann (private communication).

²⁷ H. Brooks, *Advances in Electronics*, edited by L. Marton (Academic Press Inc., New York, 1955), Vol. 7, p. 85.

²⁸ H. J. G. Meyer, Phys. Rev. **112**, 298 (1958).

²⁹ H. J. G. Meyer, J. Phys. Chem. Solids **8**, 264 (1959).

TABLE II. Evaluation of the optical deformation potential constant D_0 from measurements of the saturation drift velocity v_d at different lattice temperatures.

Author	T_{latt}	v_d (cm/sec)	D_0 (ev/cm)
Ryder ^a	77	0.9×10^7	0.37×10^9
	193	0.76×10^7	0.49×10^9
	298	0.62×10^7	0.49×10^9
Gunn ^b	300	0.55×10^7	0.43×10^9
Arthur <i>et al.</i> ^c	300	0.65×10^7	0.5×10^9
Koenig ^d	80	1.08×10^7	0.47×10^9
Koenig <i>et al.</i> ^e $\langle 100 \rangle$ sample	297	0.67×10^7	0.51×10^9

^a E. F. Ryder, Phys. Rev. **90**, 766 (1953).

^b J. B. Gunn, J. Electron. **2**, 87 (1956).

^c J. B. Arthur, A. F. Gibson, and J. W. Granville, J. Electron. **2**, 145 (1956).

^d S. H. Koenig, Proc. Phys. Soc. (London) **73**, 959 (1959).

^e S. H. Koenig, M. I. Nathan, W. Paul, and A. C. Smith, Phys. Rev. **118**, 1217 (1960).

mental data on the infrared absorption by free carriers obtained by Fan, Spitzer, and Collins.³⁰ More detailed but as yet preliminary experiments on free-carrier absorption by de Veer,³¹ evaluated on the basis of the theory of Meyer^{28,29} and Risken and Meyer,³² seem to indicate a value for D_0 much closer to our present one, $D_0 \approx 0.5 \times 10^9$ ev/cm.³¹

IV. TRANSVERSE ANISOTROPY OF HOT ELECTRONS: THE GENERAL CASE

The treatment of the last section was based on the assumption, that the intervalley scattering has no influence on the energy distribution of the electrons and was further simplified by using approximate expressions for the electron temperature (20) and for the repopulation (23). This led, as far as the anisotropy was concerned, to the temperature- and field-independent results of Figs. 3 and 5, henceforth called the limiting results. Under experimental conditions the approximations (20) and (23) may not fully apply, at least for the cold valley 1 of Fig. 2. Moreover, the finite intervalley rate may to a certain extent affect the energy distribution. Therefore, a slight dependence of the anisotropy on the electric field and the lattice temperature is to be expected.

In fact, the experimental ψ vs F curves for fixed sample orientation and fixed lattice temperature exhibit a flat maximum^{4-6,23,25,26} whose existence, after some discussion,^{33,25} is now well established.^{25,26} For $T=78^\circ\text{K}$ the experimental values of ψ_{max} , given in Fig. 5 are, as stated in Sec. III, close to the limiting results.

The reason for this particular field dependence of the anisotropy will first be discussed qualitatively. In order to do this, let us note that the anisotropy is zero if the distribution $f_0^{(i)}(\epsilon)$, and therefore the average

³⁰ H. Y. Fan, W. Spitzer, and R. J. Collins, Phys. Rev. **101**, 566 (1956).

³¹ H. J. G. Meyer and S. M. de Veer, (private communication).

³² H. Risken and H. J. G. Meyer, Phys. Rev. **123**, 416 (1961).

³³ J. B. Gunn, (private communications to S. H. Koenig cited in reference 25).

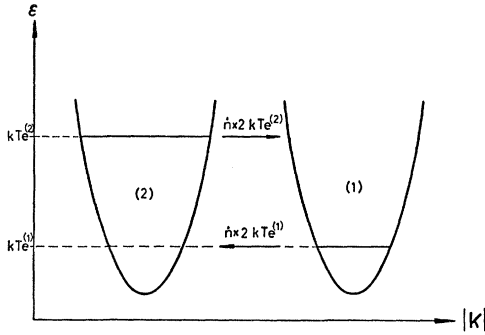


FIG. 6. Mechanism of energy transfer between different valleys.

energy $\bar{\epsilon}^{(j)}$, is the same for each j and that, roughly speaking, the anisotropy measures the quantities³⁴

$$\eta_{(i)}^{(j)} = \left| \frac{\bar{\epsilon}^{(j)}}{\bar{\epsilon}^{(i)}} - 1 \right|.$$

The initial increase of the anisotropy with increasing field strength can therefore be explained only if in the distribution (12) the better approximation (13) for the electron temperature is used instead of (20), while the influence of intervalley scattering on the energy distribution of the electrons is still neglected. Under these assumptions, the anisotropy is found to increase monotonically with increasing field strength and in the limit of high fields the limiting results of Sec. III are re-obtained. It will now be made plausible that the existence of the maximum and the final decrease of the anisotropy with increasing field strength is due to the finite intervalley rate.

Consider the two valleys of Fig. 6, whose population ratio, according to the Knudsen distribution (23), is determined by the electron temperature $T_e^{(1)}$ and $T_e^{(2)}$. In further analogy with the situation in Knudsen gases, the average energy of transfer per particle is found to be equal to $2kT_e$.³⁵ Therefore, from the point of view of the hot valley, an electron going back and forth is equivalent to an energy loss $\Delta\epsilon = 2k(T_e^{(2)} - T_e^{(1)})$ which corresponds to a number $r = \Delta\epsilon/\hbar\omega_0$ of emissive optical interactions. By this energy transfer, the importance of which increases as F^2 , the average energies of electrons in the two valleys and therefore the populations are partly equalized. In the region of high-electric fields, this gives rise to a decrease of the anisotropy with increasing electric field strength.

A quantitative description of the field and temperature dependence is obtained if the distribution

³⁴ As shown by (10a), the anisotropy is measured by $[\int f^{(i)} d\epsilon / \int f^{(i)} d\epsilon - 1]$. Insertion of (12) and (16a) shows that this quantity is practically equal to the more intuitive quantity $\eta_{(i)}^{(j)}$ used in the text.

³⁵ The energy of the intervalley phonon is neglected as compared to the average energy of the electrons as soon as the Knudsen analogy is used. For finite energy of the intervalley phonons, the average energy of transfer is in first approximation equal to $2kT_e^{(i)} - \frac{1}{2}\hbar\omega_i$.

function, (17) and (19), in which the influence of the finite intervalley rate is properly taken into account, is inserted into (10a). As we restrict ourselves to the transverse anisotropy only, factors common to all terms of the sum of the right side of (10a) can be omitted. This procedure leads after straightforward calculations to the following proportionality:

$$v_d \propto 4 \frac{\gamma^* [u^*]^2}{1 - \gamma^* [u^*]^2} F_0 + \sum_j \frac{[u^*]^2 \tilde{\alpha}^{(j)} F_0}{F_0 \tilde{\alpha}^{(j)} F_0 [u^*]^2 + m_0/m_i}, \quad (27)$$

where the second term is analogous to the vector \mathbf{S} of (25) and (26), while the first one accounts for the influence of the intervalley scattering on the drift velocity. The dimensionless variables u^* (which is proportional to the field strength) and γ^* (which is proportional to the intervalley rate constant) are defined by

$$\begin{aligned} [u^*]^2 &= \frac{2(2n_i+1)}{(2n_q+1)(2n_i+1) - \omega_i/\omega_0} \frac{E_{\langle\tau\rangle} E_{\tau_0} m_0}{(\hbar\omega_0)^2 m_i} \\ &= \frac{2(2n_i+1)}{(2n_q+1)(2n_i+1) - \omega_i/\omega_0} \\ &\quad \times \frac{1}{6} \left[\frac{e p \hbar^2 c_l}{4\pi^2 D_0 \Xi_1} \right]^2 \frac{\det \tilde{\alpha}}{m_0^3} \frac{F^2}{m_i k T_{\text{eff}}}, \quad (28) \\ \gamma^* &= \frac{(2n_q+1)(2n_i+1) - \omega_i/\omega_0}{(2n_i+1)} \frac{m_i}{m_0} \sum_j F_0 \tilde{\alpha}^{(j)} F_0 \\ &= 4 \frac{(2n_q+1)(2n_i+1) - \omega_i/\omega_0}{(2n_i+1)} \tilde{\gamma} \hbar \omega_0 \left[\frac{2}{3} + \frac{1}{3} \frac{m_i}{m_l} \right]. \quad (29) \end{aligned}$$

The range of validity of (27) is determined by the conditions that the average energy of the electrons in all valleys must be larger than the energy of an optical phonon, which, according to (28), (13), and (6), leads to $u^* > 3$. Furthermore, the deviation of the electron distribution from the original Maxwellian one must be small, which is equivalent to $\gamma^* u^{*2} \leq \frac{1}{5}$.

Equation (27) shows that the limiting results of Sec. III are to be expected in a specified range of intermediate fields only. On one side, u^* must still be so small that the first term, which describes the influence of intervalley scattering, can be neglected. The remaining sum, however, is then practically equal in direction with the vector \mathbf{S} of (25) and (26) only if $F_0 \tilde{\alpha}^{(j)} F_0 [u^*]^2 \gg m_0/m_i$. For lower values of the electric field, the anisotropy goes down on account of the incomplete saturation of the drift velocity. For higher electric fields the anisotropy also decreases because then the first term, which always points in the direction of the electric field, becomes important.

In the next section, the theory will be fitted to the experiments. By this fit, the finite intervalley rate is determined. For a comparison with the results of

Weinreich, Sanders, and White³⁶ it is expedient to express $\bar{\gamma}$ in (29) by the intervalley rate constant w_2 (see Appendix). This gives the relation

$$\gamma^* = \frac{\rho \hbar^3 \omega_0 [\det \tilde{\alpha}]^{\frac{1}{2}}}{3\sqrt{2}\pi^2 D_0^2 m_0^{\frac{3}{2}} [\hbar \omega_0]^{\frac{1}{2}}} \times \left[\frac{2}{3} + \frac{1}{3} \frac{m_t}{m_l} \right] w_2, \quad (30)$$

by which γ^* is immediately connected with the intervalley rate constant w_2 .

V. COMPARISON OF THEORY AND EXPERIMENT

In the experiments on the anisotropy of hot electrons, the angle ψ is measured as a function of the electric field strength for fixed lattice temperature and fixed sample orientation in the (110) plane. The theoretical ψ vs F characteristics can be calculated if the components $v_{d(110)}$ and $v_{d(001)}$ of the drift velocity from (27) are inserted in the relation

$$\tan \Theta = \frac{v_{d(110)}}{v_{d(001)}}. \quad (31)$$

Then, for fixed values of Θ , a surface

$$\psi = \psi(\Theta = \text{const}, \gamma^*, u^*)$$

is obtained. The contours of the particular surface $\psi(\Theta = 26^\circ, \gamma^*, u^*)$ are given in Fig. 7. The value of Θ

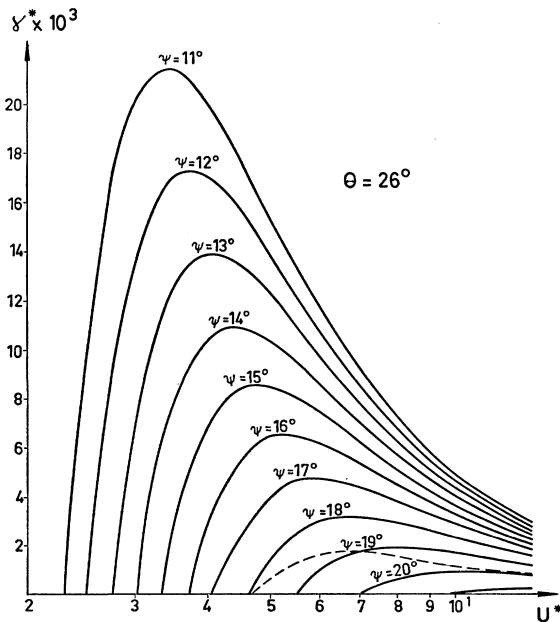


FIG. 7. Contours of the surface $\psi = \psi(\Theta = 26^\circ, \gamma^*, u^*)$.

³⁶ G. Weinreich, T. M. Sanders, and H. G. White, Phys. Rev. **114**, 33 (1959).

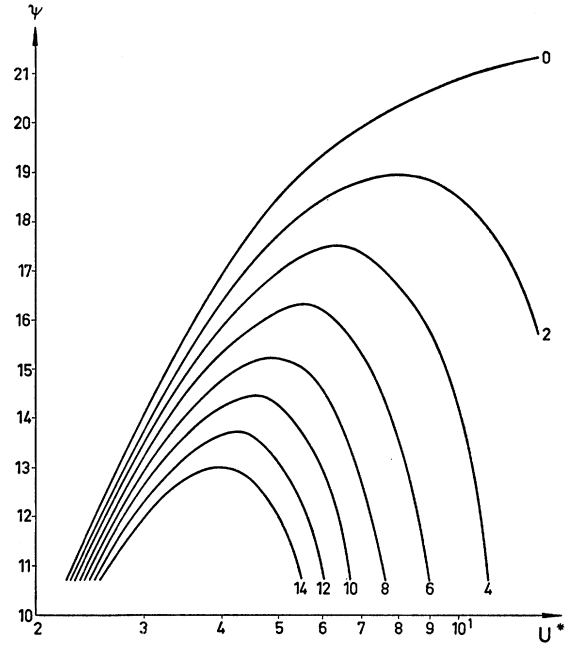


FIG. 8. Field dependence of the transverse anisotropy (Sasaki effect) for different intervalley rates. The parameter of the curves is equal to $\gamma^* \times 10^3$.

chosen corresponds to sample orientations used by Koenig²³ and Schmidt-Tiedemann.²⁶

According to (30), the experimental ψ vs F characteristics for fixed sample orientation and fixed lattice temperature correspond to the curves

$$\psi = \psi(\Theta = 26^\circ, \gamma^* = \text{const}, u^*).$$

Some plots of these curves for different values of the parameter γ^* are given in Fig. 8. For $\gamma^* \rightarrow 0$, the ψ vs u^* characteristics increase monotonically with increasing u^* and, in the limit $u^* \rightarrow \infty$, tend to the limiting results $\psi(\Theta = 26^\circ)$ of Fig. 4. For small values of u^* , the curves

$$\psi = \psi(\Theta = 26^\circ, \gamma^*, u^*)$$

and

$$\psi = \psi(\Theta = 26^\circ, \gamma^* \rightarrow 0, u^*)$$

are very similar. For larger values of u^* , however, the curves $\psi = \psi(\Theta = 26^\circ, \gamma^*, u^*)$ exhibit a maximum, whose value ψ_{max} for small values of γ^* comes close to the limiting result $\psi(\Theta = 26^\circ)$. For even higher values of u^* , the anisotropy goes down again on account of the predominance of the intervalley effect.

A comparison between the theoretical ψ vs u^* characteristics and the experimental ψ vs F characteristics can be carried out in three steps: (1) Draw the experimental ψ vs F characteristics with the same scale for the ordinate as that of Fig. 8 and the same logarithmic scale for the abscissa. Try to bring each experimental curve $\psi = \psi(\Theta = 26^\circ, T, F)$ into coincidence with

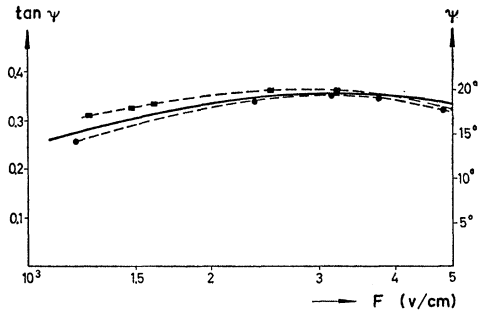


FIG. 9. Comparison of theory and experiment (Schmidt-Tiedemann). $\Theta = 26^\circ$; $T = 78^\circ\text{K}$; \blacksquare —experimental results for a 13-ohm cm sample; \bullet —experimental results for a 2.08-ohm cm sample; full curve: theory for $w_2 = 1.66 \times 10^{10} \text{ sec}^{-1}$.

a particular theoretical curve

$$\psi = \psi(\Theta = 26^\circ, \gamma^* = \text{const}, u^*)$$

by mere displacement of the two curves along their coincident abscissas-axes. If this is possible, an empirical relation $\gamma^* = \gamma^*(T)$, $u^* = u^*(T, F)$ is established. (2) Try to match the corresponding theoretical relations (28) and (30) to the empirical ones by a proper choice of the optical deformation potential constant D_0 and the intervalley rate constant w_2 . [The remaining constants in (28) and (30) are supposed to be accurately known.] (3) If this is possible, compare the values of D_0 and w_2 with the independent values from the literature which put the boundaries such that D_0 and w_2 should lie inside the limits

$$0.5 \times 10^9 \text{ ev/cm} < D_0 < 1.15 \times 10^9 \text{ ev/cm}, \\ 5 \times 10^{10} \text{ sec}^{-1} < w_2 < 2 \times 10^{11} \text{ sec}^{-1}.$$

A comparison between theory and experiment has been carried out for measurements by Koenig²³ and by Schmidt-Tiedemann,²⁶ which, apart from showing the same general features, led to quantitatively different values of ψ . The result of the comparison is shown in Figs. 9 and 10. The theoretical and the experimental ψ vs F curves can be matched satisfactorily for the

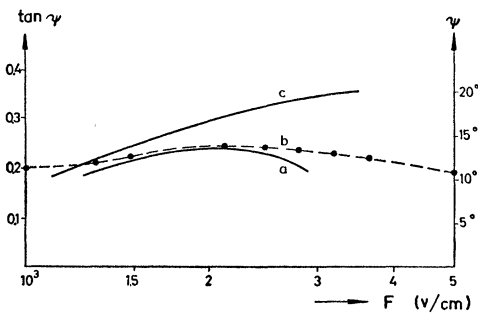


FIG. 10. Comparison of theory and experiment (Koenig). $\Theta = 26^\circ$, $T = 78^\circ\text{K}$; \bullet —experimental results; full curve a: theory for finite intervalley rate $w_2 = 10^{11} \text{ sec}^{-1}$; full curve c: theory for zero intervalley rate.

experiment by Schmidt-Tiedemann. From the fit, the following values of w_2 and D_0 :

$$w_2 = 1.66 \times 10^{10} \text{ sec}^{-1}, \quad D_0 = 0.7 \times 10^9 \text{ ev/cm},$$

are obtained. The fit between theoretical and experimental curves is less good for the measurement of Koenig. According to Koenig,³⁷ this might be due to the influence of the Gunn effect,³³ which is not excluded in his experiment. If, as in Fig. 9, only the maximum of the experimental ψ vs F curve is used for the fit, the values,

$$w_2 = 10^{11} \text{ sec}^{-1}, \quad D_0 = 10^9 \text{ ev/cm},$$

are found.

The values of w_2 and D_0 are of the correct order of magnitude in both cases. It should however be mentioned that the value of w_2 obtained from Schmidt-Tiedemann's experiment is markedly smaller than the values given by Weinreich, Sanders, and White.³⁶ The same applies for experiments of Koenig *et al.*²⁵ done for $\Theta = 30^\circ$.³⁸

VI. DISCUSSION

The transport theory of hot electrons presented in this paper was based on a special model of the band structure, viz., one type of strictly ellipsoidal valleys only. This had the advantage that for $\epsilon^{(i)} \gg \hbar\omega_0$, easily tractable expressions for the distribution function and the drift velocity could be found even for quite detailed models of the scattering processes.

The agreement between this theory and the experiments for *n*-Ge as presented in Secs. III–V especially the explanation of the field dependence of the Sasaki effect, gives evidence that the model and the further approximations inherent in this and the previous treatment⁷ are not too unrealistic for the experimental conditions under study. It is nevertheless worthwhile to discuss in more detail the question of the reliability of the theory.

We first note that each measurement of the anisotropy of hot electrons is at the same time a thermometric measurement, on account of Fig. 8 and the relation

$$kT_e^{(i)} = \left\{ \frac{(2n_q + 1)(2n_i + 1) - \omega_i/\omega_0}{2(2n_i + 1)} [u^*]^2 F_0 \tilde{\alpha}^{(i)} F_0 + n_q + \frac{1}{2} \right\} \hbar\omega_0, \quad (32)$$

by which the variable u^* is related to the electron temperature in the zeroth approximation, (12) and (13), of the distribution function.

³⁷ S. H. Koenig (private communication).

³⁸ The theoretical values of ψ calculated by J. Yamashita and K. Inoue, [J. Phys. Chem. Solids **12**, 1 (1960)] and M. Shibuya and W. Sasaki, [J. Phys. Soc. Japan **15**, 207 (1960)] with Weinreich's value of w_2 are too small as compared to the experiments of Sasaki *et al.*,⁴⁻⁶ although these experiments are probably influenced by the Gunn effect.

The value $\psi_{\max}=19^\circ$, found in Schmidt-Tiedemann's experiment, corresponds to $u^*=8.4$ (C.f. Fig. 8). Therefore the electron temperatures in the valleys 1-4 of Fig. 2 are found to be

$$\begin{aligned} T_e^{(1)} &= 540^\circ\text{K}, \\ T_e^{(2)} &= T_e^{(3)} = 3700^\circ\text{K}, \\ T_e^{(4)} &= 4200^\circ\text{K}. \end{aligned}$$

The electron temperatures in the valleys 2-4 are very high. One may therefore have some doubt about the assumption of constant effective masses in these "hot valleys"^{39,40} and about the assumption that the higher, nonequivalent valleys play no part in hot-electron effects.^{41,42} If we postpone this question, we remark that, on the other hand, the temperature of the cold valley 1 is relatively low. The use of the distribution function (17) and (19), in which the determination of K_j from the intervalley balance was based on the assumption $\hbar\omega_i/kT_e^{(1)} \ll 1$, is therefore also open to criticism. In fact, a small relative error in the large first term of (17) may already be of the same order of magnitude as the small corrections, linear in the intervalley rate constant. A fit between theory and experiment is therefore liable to give only the order of magnitude of the intervalley rate constant w_2 . The errors coming from the cold valley can in principle be eliminated by a better approximation, which, however, leads to very complicated expressions. It is therefore easier, and equally instructive, to make the approximation even worse by using the distribution (17) and (19) with $\beta_j\hbar\omega_i=0$. This deliberate deterioration of the approximation has no influence on the form of the ψ vs u^* characteristics in Fig. 8, for Eq. (27) is re-obtained. However, the relation between u^* and F , γ^* and w_2 is now different for, as a consequence of $\beta_j\hbar\omega_i=0$, ω_i in Eqs. (28) and (30) is now set equal to zero. The fit between experiment and theory, based on this deliberate deterioration of the approximation, will therefore lead to a value of D_0 which is approximately one half and to a value of w_2 approximately one quarter of the values obtained in the last section. On the other hand, as shown by (32), the electron temperatures would be four times as high as before.

We therefore conclude that the form of the theoretical ψ vs F curve is due only to the simple physical picture given in Fig. 6, and is not very sensitive to the accuracy of the approximations. However, the quantitative interpretation in terms of intervalley rate constant and electron temperature is very distinctly influenced by more or less accurate approximations. The same seems

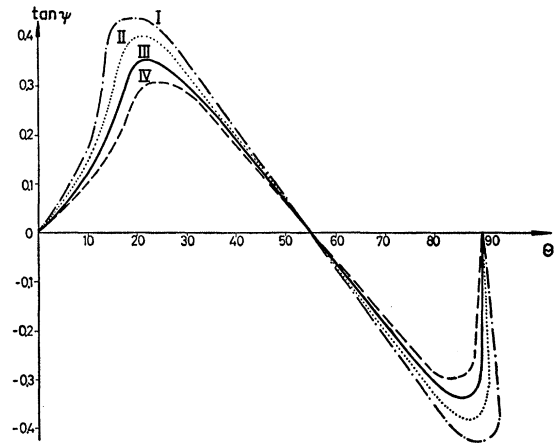


FIG. 11. Anisotropy angle ψ vs sample orientation Θ .

- I. $u^* = \infty$, $\gamma^* = 0$.
- II. $u^* = 7$, $\gamma^* = 0$.
- III. $u^* = 7$, $\gamma^* = 2 \times 10^{-3}$.
- IV. $u^* = 7$, $\gamma^* = 4 \times 10^{-3}$.

to apply for the hot valleys and even if the influence of the nonequivalent valleys is taken into account as proposed by Stratton. Then, for such values of the field, where the average energy of an electron in some of the $\langle 111 \rangle$ valleys is higher and in the other ones lower than the energy of the minimum of the high valleys, the anisotropy-enhancing mechanism of Koenig *et al.* will act. For higher fields, where the average energy of the electrons in all $\langle 111 \rangle$ valleys is higher than the minimum of the nonequivalent valleys, the anisotropy will decrease with increasing field. The reason for this is, on the one hand, the appreciable population of the high valleys, on the other hand, the scattering between nonequivalent valleys by which the average energies of the electrons in different valleys is

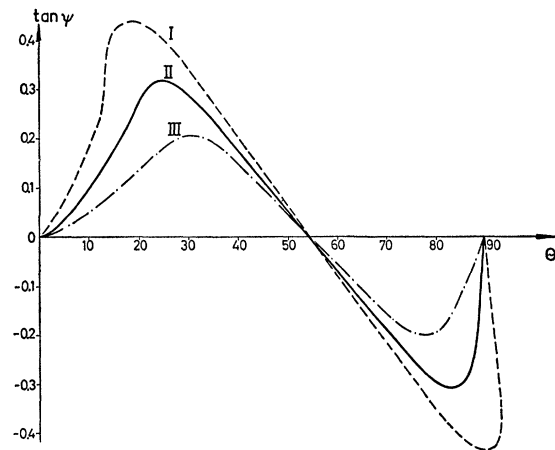


FIG. 12. Anisotropy angle ψ vs sample orientation Θ .

- I. $u^* = \infty$, $\gamma^* = 0$.
- II. $u^* = 11$, $\gamma^* = 2 \times 10^{-3}$.
- III. $u^* = 11$, $\gamma^* = 4 \times 10^{-3}$.

³⁹ F. Herman, Proc. Inst. Radio Engrs. **43**, 1703 (1955).

⁴⁰ M. Cardona, W. Paul, and H. Brooks, Helv. Phys. Acta **33**, 329 (1960).

⁴¹ M. I. Nathan, W. Paul, and H. Brooks, Phys. Rev. **123**, 391 (1961).

⁴² R. Stratton, J. Electronics **5**, 157 (1958).

very efficiently equalized. In summarizing the foregoing discussion, we may state that for experiments with a sample orientation $\Theta = 26^\circ$ the assumption of the theory may not fully apply; that, however, the results of the theory are not very sensitive.

For a more conclusive check of the theory and a more accurate determination of the intervalley rate constant, we propose measurements of the anisotropy near $\Theta = 90^\circ$, where in a specified region of the electric field all our assumptions apply and where, furthermore, as is shown by Figs. 11 and 12, the anisotropy is very sensitive to the intervalley rate constant.

$$\left[\frac{\partial f_0^{(i)}}{\partial t} \right]_{\text{int}} = A \sum_{i \neq j} \left\{ \left(\frac{\epsilon}{\hbar\omega_0} + 1 \right) \left[(n_i + 1) f_0^{(l)}(\epsilon + \hbar\omega_i) - n_i f_0^{(i)}(\epsilon) \right] + \left(\frac{\epsilon}{\hbar\omega_0} - 1 \right) \left[n_i f_0^{(l)}(\epsilon - \hbar\omega_i) - (n_i + 1) f_0^{(i)}(\epsilon) \right] \right\}, \quad (\text{A1})$$

where $[\partial f_0^{(i)}/\partial t]_{\text{int}}$ is the rate of change of the distribution function due to intervalley scattering, and

$$A = \frac{\sqrt{2} 4\pi^2 D_i^2 m_0^{\frac{3}{2}} (\hbar\omega_i)^{\frac{1}{2}}}{\rho \hbar^3 \omega_i [\det \tilde{\alpha}]^{\frac{1}{2}}} \quad (\text{A2})$$

are applied to the experiment of Weinreich *et al.* In this experiment, electrons in the two different pairs of valleys behave like particles with positive and negative acoustical charges q in an acoustical potential Φ . The rate of transfer of positive acoustical particles into negative acoustical particles can be obtained if the four-equation (A1) is collected in pairs and the Boltzmann average is performed. Taking the asymptotic behavior of the modified Hankel function $K_1(\hbar\omega_i/kT)$

ACKNOWLEDGMENTS

The authors thank Professor D. Polder and H. J. G. Meyer (Eindhoven), Professor W. Franz, and Dr. K. J. Schmidt-Tiedemann for helpful and stimulating discussions. Special thanks are due to Dr. K. J. Schmidt-Tiedemann for making available his results prior to publication. The assistance of D. Heese with numerical calculations was indispensable.

APPENDIX I

The relation (30) between γ^* and the intervalley rate constant w_2 can be derived if

for $\hbar\omega_i/2kT \ll 1$ properly into account, the rate of transfer

$$d\delta n_+/dt = d\delta n_-/dt = -8A \exp(-\hbar\omega_i/kT) \delta n_+ \quad (\text{A3})$$

is found, where δn_+ is the deviation of the population of the positive pair of valleys from their equilibrium population,

$$n_{+0} = n_0(1 - q\Phi/kT).$$

Comparison of (A3) with Eqs. (3.6) and (8.4) of Weinreich, Sanders, and White shows that

$$w_2 = 3A. \quad (\text{A4})$$

Insertion of (A2) and (18) gives (30).

Low-Temperature Specific Heat of Ti Alloys with CsCl-Type Ordered Structure

E. A. STARKE, JR., C. H. CHENG, AND PAUL A. BECK

University of Illinois, Urbana, Illinois

(Received January 2, 1962)

A continuous solid-solution field extends at 1100°C in the Ti-Fe-Co ternary system between the CsCl-type binary phases TiFe and TiCo. In the Ti-Co-Ni ternary system a similar solid-solution field extends at 1175°C from TiCo at least to $\text{Ti}_4\text{Co}_3\text{Ni}$.

The electronic specific heat coefficient of TiFe-TiCo alloys and of $\text{Ti}_4\text{Co}_3\text{Ni}$ was found to have a large peak at the same average electron concentration where the γ peak for the bcc Cr-Fe alloys occurs.

INTRODUCTION

A STUDY of the electronic specific heat at low temperatures of bcc alloys of first long-period transition elements¹ indicated that in different alloy

systems the variation of the electronic specific heat with the average electron concentration (the average number of electrons outside the closed shells of the various component atoms) is very similar. This similarity suggests that, at least in a first approximation, these alloys may be described in terms of a nearly rigid $3d$ -band model.

¹ C. H. Cheng, C. T. Wei, and Paul A. Beck, Phys. Rev. **120**, 426 (1960).